

RESEARCH

Open Access



Radiomic-based models are able to predict the pathologic response to different neoadjuvant chemotherapy regimens in patients with gastric and gastroesophageal cancer: a cohort study

Annamaria Agnes^{1,2}, Luca Boldrini^{1,3}, Federica Perillo¹, Huong Elena Tran³, Maria Gabriella Brizi^{1,3}, Riccardo Ricci^{1,4}, Jacopo Lenkowicz³, Claudio Votta³, Alberto Biondi^{1,2*}, Riccardo Manfredi^{1,3}, Vincenzo Valentini^{1,3}, Domenico M. D'Ugo^{1,2} and Roberto Persiani^{1,2}

Abstract

Background There is a clinical need to identify early predictors for response to neoadjuvant chemotherapy (NAC) in patients with gastric and gastroesophageal junction cancer (GC and GEJC). Radiomics involves extracting quantitative features from medical images. This study aimed to apply radiomics to build prediction models for the response to NAC.

Methods All consecutive patients with non-metastatic GC and GEJC undergoing NAC and surgical resection in an Italian high-volume referral center between 2005 and 2021 were considered eligible. In patients selected, the CT scans performed upon staging were reviewed to segment the tumor and extract radiomic features using MODDICOM. The primary endpoint was to develop and validate radiomic-based predictive models to identify major responders (MR: tumor regression grade TRG 1–2) and non-responders (NR: TRG 4–5) to NAC. Following an initial feature selection, radiomic and combined radiomic-clinicopathologic prediction models were built for the MR or NR status based on logistic regressions. Internal validation was performed for each model. Radiomic models (in the entire case series and according to NAC regimens) were evaluated using the receiver operating characteristic area under the curve (AUC), sensitivity, and negative predictive value (NPV).

Results The study included 77 patients undergoing NAC and subsequent tumor resection. The MR prediction model after all types of NAC (AUC of 0.876, CI 95% 0.786–0.966, sensitivity 83%, and NPV 96%) was based on a statistical feature. The models predicting NR among patients undergoing epirubicin with cisplatin and fluorouracil (ECF), epirubicin with oxaliplatin and capecitabin (EOX), or fluorouracil with oxaliplatin and docetaxel (FLOT) (AUC 0.760,

*Correspondence:
Alberto Biondi
alberto.biondi@policlinicogemelli.it

Full list of author information is available at the end of the article



© The Author(s) 2025. **Open Access** This article is licensed under a Creative Commons Attribution-NonCommercial-NoDerivatives 4.0 International License, which permits any non-commercial use, sharing, distribution and reproduction in any medium or format, as long as you give appropriate credit to the original author(s) and the source, provide a link to the Creative Commons licence, and indicate if you modified the licensed material. You do not have permission under this licence to share adapted material derived from this article or parts of it. The images or other third party material in this article are included in the article's Creative Commons licence, unless indicated otherwise in a credit line to the material. If material is not included in the article's Creative Commons licence and your intended use is not permitted by statutory regulation or exceeds the permitted use, you will need to obtain permission directly from the copyright holder. To view a copy of this licence, visit <http://creativecommons.org/licenses/by-nc-nd/4.0/>.

CI 95% 0.639–0.882), oxaliplatin-based chemotherapy (AUC 0.810, CI 95% 0.692–0.928), and FLOT (AUC 0.907, CI 95% 0.818–0.995) were based on statistical, morphological and textural features.

Conclusions The developed radiomic models resulted promising in predicting the response to different neoadjuvant chemotherapy strategies. Once further implemented on larger datasets, they could be valuable and cost-effective instruments to target multimodal treatment in patients with GC.

Keywords Gastric cancer, Radiomics, Neoadjuvant therapy, Predictive models, Precision oncology

Introduction

The administration of perioperative chemotherapy in association with radical surgical resection represents the Western standard of care for patients with locally advanced gastric and gastroesophageal cancer (GC and GEJC). Previous phase III randomized clinical trials have validated the benefits of combined perioperative regimens in this population [1–3]. Perioperative chemotherapy includes both a neoadjuvant and an adjuvant phase; the rationale for the administration of the neoadjuvant phase is the possibility of downstaging, increasing the R0 resection rate, and improving compliance when compared to postoperative therapy. Moreover, the administration of neoadjuvant therapy gives the possibility of measuring the response of the disease to the chemotherapeutic agents in advance and, in some cases, a complete response may also be achieved (reported as high as 16% in the AIOM-FLOT4 trial) [3]. However, it is still not predictable if patients undergoing neoadjuvant therapy will be major responders and, therefore, if they could benefit from a prolonged neoadjuvant regimen. Moreover, 20–38% of patients have been reported as non-responders to neoadjuvant chemotherapy, with poor or null tumor regression at the definitive pathologic exam [4, 5]. Concerns have been raised for these patients about whether the administration of neoadjuvant therapy could delay a timely surgical treatment, cause immunosuppression, or favor the selection of undifferentiated or chemoresistant clones [6–8]. The status of major responder or non-responder to neoadjuvant chemotherapy is not univocally predictable based on conventional pathologic classifications (i.e., Lauren's and WHO), due to the heterogeneous biologic behavior of GC and GEJC in the same category. Instead, classifications based on genomics or molecular features, that have the theoretical advantage of being univocal and best correlated with GC and GEJC biologic behavior, are expensive and not easily applicable in routine clinical practice. Additionally, biomarker expression can vary between biopsies and over time, complicating treatment decisions [9–11]. Traditional imaging markers, on the other hand, often lack precision and may not detect early treatment responses [12].

Radiomics is a specific image-based data mining approach that extracts and analyzes features from medical bio-imaging to acquire information inaccessible

through the standard human-eye image analysis. Given its provision of a comprehensive, quantitative, and non-invasive analysis of complex imaging patterns, it may be helpful to realize predictive models and clinical decision-making tools [13]. Specific radiomic signatures have already been related to GC-specific prognosis, within models that showed a better predictive performance than models based on clinical or pathologic variables alone [14, 15]. Such strategies have been proposed to predict the efficacy of adjuvant therapy according to pathologic and immunopathological characteristics, while only a few preliminary studies have attempted to identify a radiomic signature associated with the effectiveness of neoadjuvant therapy [4].

Based on the clinical need to identify early and valuable predictors for response to chemotherapy, this study aimed to apply radiomics to identify image features associated with chemosensitive and chemoresistant GC and GEJC phenotypes and to exploratively develop radiomic-based prediction models to prove their feasibility.

Methods

Study design and patient selection

This study was designed and conducted according to the TRIPOD guidelines (category 1b) [16] at the Fondazione Policlinico Universitario A. Gemelli IRCCS, Rome, Italy. We selected for inclusion in the study all patients with histologically proven GC and GEJC undergoing preoperative chemotherapy and surgical resection in the General Surgery Unit and the General Surgery and Transplant Unit between January 2005 and April 2021. Patients with Siewert 1 GEJC, patients undergoing preoperative chemotherapy with the adjunct of a biologic drug (i.e., trastuzumab, regorafenib) or those undergoing preoperative chemoradiotherapy, and patients without the availability of the staging CT scan or insufficient quality of the images in terms of sequences performed, pixel spacing, and slice thickness homogeneity (> 5 mm) and absence of artifacts, were excluded.

Informed consent for the treatment and data privacy and protection were obtained from all study participants. The study received approval from our Institutional Research Committee and was registered on clinicaltrials.gov (NCT06044961). All procedures were performed

following the 1964 Helsinki Declaration and its later amendments.

Data were collected from the medical records and included: age, gender, location, involvement of the gastroesophageal junction (GEJ), Lauren histology, clinical staging (serosal invasion-cT4, cN+-nodal disease, cM+), type of upfront therapy, type of resection, pathological staging (ypTNM/A)CC 8th), and pathologic tumor response, see below.

Preoperative chemotherapy and indications for surgical resection

All patients referred to the Institution for GC and GEJC treatments undergo endoscopy with biopsy and are staged using contrast-enhancement computer tomography (CT) of the thorax and the abdomen. Neoadjuvant chemotherapy is considered for patients with locally advanced (> T2 or node-positive) potentially resectable GC and GEJC, with no evidence of distant metastases (cM0), as previously detailed [17]. Moreover, stage IV patients with oligometastatic disease, who had a downstaging or stable disease after chemotherapy, were evaluated for conversion surgery [18].

Neoadjuvant chemotherapy consists of different platinum-based chemotherapy regimens in combination with pyrimidine analogs and anthracyclines or taxanes. In our institution, ECF (epirubicin, cisplatin, fluorouracil) and EOX (epirubicin, oxaliplatin, capecitabine) and CF (cisplatin, fluorouracil) were administered as the standard neoadjuvant regimen before 2018 (using CF in patients not deemed fit to receive a full ECF/EOX regimen) and FLOT is administered as the standard neoadjuvant regimen from 2018 (using FOLFOX in patients not deemed fit to receive FLOT chemotherapy). Patients with Siewert II GEJC were alternatively treated with chemotherapy or chemoradiotherapy before the implementation of the FLOT regimen in 2018; since then, they have been treated with neoadjuvant chemotherapy (FLOT) only. Surgery is performed after 3 to 4 weeks from the end of chemotherapy and consists of total gastrectomy for proximal tumor locations and subtotal gastrectomy for distal tumor locations if a 5 to 6 cm safety margin is present. Ivor-Lewis esophagectomy is considered for selected patients with Siewert 2 GEJC. Oligometastatic disease is treated by intraoperative evaluation and resection/cytoreduction. Patients with oligometastatic peritoneal disease are evaluated for cytoreduction +/- HIPEC (hyperthermic intraperitoneal chemotherapy).

Radiomic data collection and feature extraction

All CT scans performed upon diagnosis and before the neoadjuvant therapy of included patients were reviewed. If the CT scans were not available in the Institutional radiological archive (picture archiving and

communication system - PACS system), the patients were contacted, and images were obtained and uploaded in the PACS.

All contrast CT scans were imported on a dedicated workstation (Eclipse, Varian Medical Systems, Palo Alto, CA, USA) designed for advanced segmentation of biomedical images. The region of interest (ROI), corresponding to the gross tumor volume (GTV) was delineated slice by slice on portal-phase images. All the ROIs were manually segmented by one junior (FP) and then independently reviewed by one senior radiologist (MGB) with 4 and >25 years of experience, respectively (Supplementary Fig. 1). The feature extraction was performed using MODDICOM (<https://github.com/kbolab/moddicom>), an R library designed to perform radiomic analysis by the Radiomics Research Core facility of the Fondazione Policlinico Universitario "A. Gemelli" IRCCS, Rome, Italy fully compliant with the Image Biomarker Standardisation Initiative (IBSI) recommendations [19, 20].

A total of 217 radiomic features belonging to three families (statistical, morphological, and textural) were extracted from the ROI. Statistical features characterize the properties of the gray-level histogram within the ROI using statistical measures. Morphological features describe the geometric properties of the ROI, while textural features characterize the local distribution of the gray levels within the ROI.

Outcomes of interest

The primary endpoint of this study was to develop radiomic-based predictive models able to identify major responders (MR) and non-responders (NR) to neoadjuvant chemotherapy, overall and according to different chemotherapy schemes. The pathological tumor response to chemotherapy was evaluated using the Mandard tumor regression grade (TRG) criteria: patients were classified as MR (TRG 1–2), non-MR (TRG 3–5), responders (TRG 1–3) and NR (TRG 4–5) [21]. For this study, all available slides were reviewed by a single senior pathologist (RR) expert in pathology of the upper gastrointestinal tract with more than 25 years of experience.

Statistical analysis and radiomic models

The statistical analysis was performed in RStudio, version 3.6.3 (RStudio Team (2020). RStudio: Integrated Development for R. RStudio, PBC, Boston, MA URL <http://www.rstudio.com/>) and IBM SPSS Statistics for Macintosh, version 25 (IBM Corp., Armonk, N.Y., USA). Radiomics modeling was performed in RStudio. A database was created combining the radiomic features with the clinicopathologic parameters and the outcome data.

Categorical variables were represented as frequencies and continuous variables as mean and median with standard deviation and range, respectively. The chi-squared

and Fisher exact tests were employed to compare categorical variables, while the t-test and Mann-Whitney-Wilcoxon test were employed to compare continuous variables, as appropriate.

- Feature selection: initial radiomic feature selection was performed with the univariate analysis via Mann-Whitney-Wilcoxon test ($p < 0.05$) and followed by application of the Pearson correlation coefficient (targeted as ≤ 0.9) or of the Boruta algorithm for machine learning feature selection (R package: *Boruta_1.3.tar.gz*) to obtain the minimum set of informative feature and reduce the risk of overfitting [22]. Pearson correlation allowed to eliminate highly correlated variables to reduce redundancy and multicollinearity for the MR model, while the Boruta algorithm permitted to ensure that only relevant predictors were retained for the NR model.
- Model development: The selected features were used as variables in a stepwise unpenalized logistic regression modeling approach based on the Akaike Information Criteria (AIC) to create the radiomic prediction model. Tested clinicopathological variables for the development of combined radiomic-clinicopathologic models included: age, gender, involvement of the GEJ, clinical TNM staging, histotype according to Lauren, and presence of signet-ring-cell (SRC) features. To determine the association of the clinicopathologic variables with the pathologic outcomes, the Fisher exact test was employed to select variables significant at < 0.05 , that were subsequently included in a combined radiomic-clinicopathologic multivariable logistic regression model. Model fitting was performed using the bias-reduction method developed by Firth [23] for the predictions of rare events. The goodness of fit for all the logistic regression models was assessed with the Hosmer-Lemeshow test, where $p > 0.05$ indicated that there are no significant differences between observed outcomes (i.e., the actual data) and model predictions. This statistical test is particularly useful for evaluating how well the logistic regression model predicts probabilities across different ranges of predicted outcomes. Calibration plots were constructed by plotting observed outcome probabilities against model-predicted outcome probabilities, with 95% confidence intervals (CI95%) set for the calibration belt (r package: *givitiR_1.3.tar.gz*). These calibration plots graphically assess how well the predicted probabilities from the model match the actual observed outcomes, showing whether the predicted probabilities are accurate across different levels of predicted risk. Discrimination was assessed with the

area under the curve (AUC) of receiver operating characteristic (ROC) curves and model performance metrics, namely accuracy, sensitivity, specificity, positive predictive value, and negative predictive value. These metrics summarize the model's ability to discriminate between positive and negative classes, assigning higher probabilities to the positive class and lower probabilities to the negative class. CI95% for the AUC was computed with 2000 stratified bootstrap replicates of the predictions using the *ci.auc* function. The cut-offs and CI95% for model performance measures were calculated by Youden's J statistics, and Jeffreys method for small sample sizes, respectively [24].

- Internal validation: internal validation was performed by applying the bootstrap resampling method to the data (1000 iterations) according to the TRIPOD guidelines [16]. This method assesses the degree of optimism in the predictive performance of the developed model and estimates how well the model is likely to perform when applied to other samples. A logistic regression model was developed for each bootstrap sample to calculate the optimism-corrected AUC as the discrimination metric to adjust for potential overfitting of the model [16]. The CI 95% for the optimism-corrected AUC was obtained by using the percentile method. Model calibration was tested with the *calibrationbelt* function [25].

Results

From an initial population of 718 patients with GC and GEJC presenting to the surgical attention during the study period, 132 underwent neoadjuvant chemotherapy and subsequent resection. Among these patients, according to the inclusion and exclusion criteria (Supplementary Fig. 2), 77 were selected for this study. The clinicopathologic characteristics of these patients are presented in Table 1.

Detailed information on the chemotherapy regimens applied and on the corresponding TRGs are presented in Table 2.

Predictive model for the identification of MR vs. non-MR

Only one model was calculated, including patients undergoing all types of chemotherapy. In this model, the feature selected by the Pearson correlation and subsequent AIC was the "F_stat.10thpercentile", a statistical feature related to the 10th percentile of the intensity-histogram within the ROI (Fig. 1). Among the clinicopathologic variables, the Lauren classification and the presence of SRC features were selected as those better correlated with MR. The radiomic-clinicopathologic model resulting from the multivariable logistic regression model ($n = 73$ patients – 4 excluded due to missing

Table 1 Clinicopathological characteristics of MRs, responders and NRs

Variable	MRs - TRG 1–2 (n = 12)	Non-MRs - TRG 3–5 (n = 65)	P value	Responders - TRG 1–3 (n = 38)	NRs - TRG 4–5 (n = 39)	P value
Age (mean ± SD)	63+11	66+11	0.446	64 +- 9	63+12	0.885
Gender, n (%)			0.526			0.935
Male	5 (41.7)	21(32.3)		13 (34.2)	13 (33.3)	
Female	7 (58.3)	44(67.7)		25 (65.8)	26 (66.7)	
Tumor location	3 (25)	17 (26.2)	0.505			0.101
Proximal	0 (0)	10 (15.4)		14 (36.8)	6 (15.4)	
Middle	8 (66.7)	33 (50.8)		4 (10.5)	6 (15.4)	
Distal	1 (8.3)	5 (7.7)		16 (42.1)	25 (64.1)	
Whole stomach				4 (10.5)	2 (5.1)	
GEJ involvement			0.498			0.087
No	5 (41.7)	34 (52.3)		23 (60.5)	16 (41)	
Yes	7 (58.3)	31 (47.7)		15 (39.5)	23 (59)	
cT4			0.657			0.202
No	6 (50)	37 (56.9)		24 (63.2)	19 (48.7)	
Yes	6 (50)	28 (43.1)		14 (36.8)	20 (51.3)	
cN1			0.002			0.177
No	8 (66.7)	13 (20)		13 (34.2)	8 (20.5)	
Yes	4 (33.3)	52 (80)		25 (65.8)	31 (79.5)	
cM+			0.441			0.535
No	11 (91.7)	50 (76.9)		29 (76.3)	32 (82.1)	
Yes	1 (8.3)	15 (23.1)		9 (23.7)	7 (17.9)	
Type of resection			0.677			0.098
Subtotal	4 (33.3)	20 (30.8)		16 (42.1)	8 (20.5)	
Total	8 (66.7)	41 (63.1)		21 (55.3)	28 (71.8)	
Ivor-Lewis esophagectomy	0 (0)	4 (6.1)		1 (2.6)	3 (7.7)	
Lauren histotype			0.072*			0.219*
Intestinal	8 (66.7)	26 (40)		20 (52.6)	14 (35.9)	
Mixed	1 (8.3)	14 (21.5)		6 (15.8)	9 (23.1)	
Diffuse	1 (8.3)	23 (35.4)		9 (23.7)	15 (38.5)	
Data not available	2 (16.7)	2 (3.1)		3 (7.9)	1 (2.5)	
SRC features			0.003*			0.244*
No	12 (100)	33 (50.7)		25 (65.8)	22 (56.4)	
Yes	0 (0)	28 (43.1)		11 (28.9)	17 (43.6)	
Data not available	0 (0)	4 (6.1)		2 (5.3)	0 (0)	
yp Stage			0.001			0.005
complete response	4 (33.3)	0 (0)		4 (10.5)	0 (0)	
I	5 (41.7)	7 (10.8)		10 (26.3)	2 (5.1)	
II	2 (16.7)	18 (27.7)		10 (26.3)	10 (25.6)	
III	1 (8.3)	25 (38.5)		7 (18.4)	19 (48.7)	
IV	0 (0)	15 (23.1)		7 (18.4)	8 (20.5)	

* p values calculated excluding the missing values. MRs: major responders; NRs: non-responders; TRG: tumor regression grade according to Mandard; GEJ: gastroesophageal junction; SRC: signet-ring cell

clinicopathological data, Supplementary Table 1) selected “F_stat.10thpercentile” and the presence of SRC features as significant predictor variables, showing a Hosmer-Lemeshow p-value of 0.495. The ROC AUC of the model was 0.876 (CI 95% 0.786–0.966). The calibration linear equation of the model was $y = (-)0.048 + 1.372 * x$. After bootstrap resampling, the optimism-corrected ROC AUC (CI 95%) was 0.871 (0.769–0.958), and the calibration belt did not show a significant deviation from the ideal calibration (Fig. 2) (Table 3).

Predictive models for the identification of NR vs. responders

Firstly, we tested the model for all chemotherapy regimens (CF + ECF/EOX + FOLFOX + FLOT). (n = 77 patients, Supplementary Table 2, Supplementary Fig. 3). In this model, the feature selected by the Boruta algorithm and AIC was: “F_stat.energy”, a statistical feature. The resulting logistic regression model had a Hosmer-Lemeshow p of 0.519 and a ROC AUC of 0.725 (0.610–0.839) (Table 3). In patients undergoing ECF/

Table 2 Types of chemotherapy administered to the study population and corresponding TRG values

Type of chemotherapy	TRG1	TRG2	TRG3	TRG4	TRG5
FLOT, n=40	2 (50)	5 (62.5)	11 (42.3)	18 (58.1)	4 (50)
FOLFOX, n=10	1 (25)	1 (12.5)	3 (11.5)	2 (6.5)	3 (37.5)
ECF, n=18	0 (0)	1 (12.5)	9 (34.6)	8 (25.8)	0 (0)
EOX, n=3	0 (0)	1 (12.5)	1 (3.8)	0 (0)	1 (12.5)
CF, n=6	1 (25)	0 (0)	2 (7.7)	3 (9.7)	0 (0)

TRG: tumor regression grade according to Mandard; FLOT: fluorouracil, leucovorin, oxaliplatin and docetaxel; FOLFOX: fluorouracil, leucovorin, and oxaliplatin; ECF: epirubicin, cisplatin and fluorouracil; EOX: epirubicin, oxaliplatin and capecitabine; CF: cisplatin and fluorouracil

EOX + FLOT (61 patients), the feature selected by the Boruta algorithm and subsequent logistic regression was again: “F_stat.energy”. The model constructed with this radiomic feature (n=61 patients, Supplementary Table 3) had a Hosmer-Lemeshow p of 0.468 and a ROC AUC of 0.760 (CI 95% 0.639–0.882). The calibration linear equation of this model was $y = (-)0.02943 + 0.97936 * x$. After bootstrap resampling, the optimism-corrected ROC AUC (CI 95%) was 0.762 (0.621–0.871) and the calibration belt did not show a significant deviation from the ideal calibration (Fig. 3; Table 3). Also, in 53 patients treated with oxaliplatin-based chemotherapy (EOX + FOLFOX + FLOT), the features selected by the Boruta algorithm subsequent stepwise AIC were: “F_morph.volume”, a morphological feature, and “F_szm.hgze”, a textural feature based on the gray level size zone matrix (GLSZM), including the counts of the number of groups of linked pixels with the same intensity value. The logistic regression model constructed with these radiomic features (n=53 patients, Supplementary Table 4) had a Hosmer-Lemeshow p of 0.856 and a ROC AUC of 0.810 (CI 95% 0.692–0.928). The calibration linear equation of the model was $y = (-)0.054 + 1.112 * x$. After bootstrap resampling, the optimism-corrected ROC (CI

95%) was 0.793 (0.692–0.927), and the calibration belt did not show a significant deviation from the ideal calibration (Fig. 4; Table 3). We therefore explored patients treated exclusively with FLOT chemotherapy (n=40 patients). In this model, the features selected by the Boruta algorithm and subsequent stepwise AIC were: “F_morph.volume”, a morphologic feature and “F_szm_2.5D.szhge”, a textural feature based on the GLSZM. The logistic regression model constructed with these radiomic features (Supplementary Table 5) had a Hosmer-Lemeshow p of 0.291 and a ROC AUC of 0.907 (CI 95% 0.818–0.995). The calibration linear equation of the model was $y = (-)0.059 + 1.085 * x$. After bootstrap resampling, the optimism-corrected ROC AUC was 0.892 (0.817–0.987), and the calibration belt did not show a significant deviation from the ideal calibration (Fig. 5; Table 3).

Discussion

In this study, we developed a set of radiomic models for the prediction of pathologic response after neoadjuvant chemotherapy in locally advanced gastric and GEJ cancer, aiming to identify MR to neoadjuvant therapy (TRG 1–2) in the first model and NR (TRG 4–5) in the following ones.

The use of predictive approaches for response to neoadjuvant chemotherapy has gained attention due to the heterogeneous nature of GC and GECJ and to the urgent need for more personalized treatment strategies. Models based on clinical factors, tumor markers, or traditional imaging fail to account for the molecular heterogeneity of gastric cancer and do not reliably predict chemosensitivity [12, 26, 27]. Models based on molecular/genomic approaches are promising as they could address the heterogeneity of gastric cancer but are still under investigation and their introduction in the clinical practice is limited by the high costs and need for specialist facilities

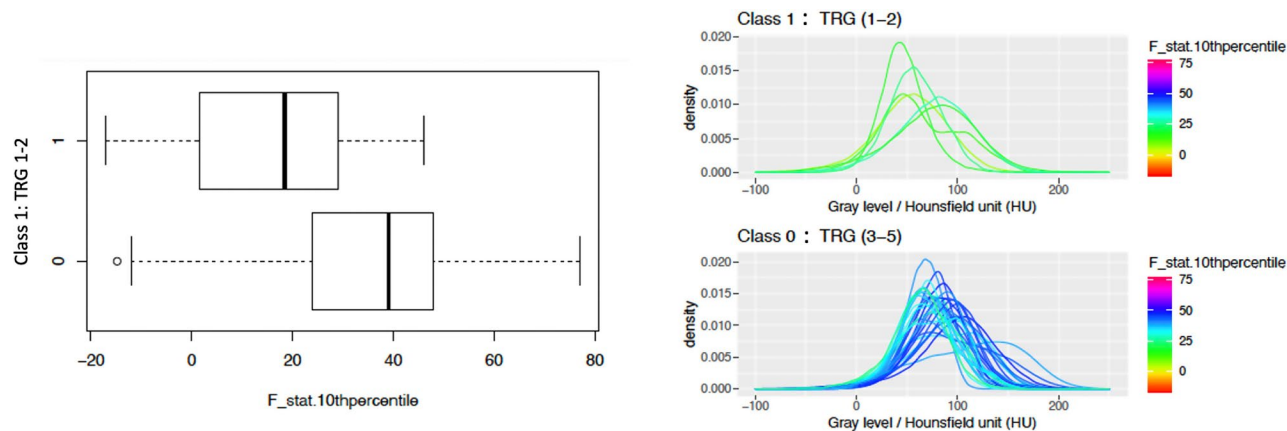


Fig. 1 Left side - boxplot showing the distribution of F_stat.10thpercentile for the two classes (class 1: major responders - MR (TRG 1–2), class 0: non-MR (TRG 3–5)); right side - density plots showing the distributions of gray levels, colors represent the F_stat.10thpercentile value of each ROI within the interquartile range for the two classes

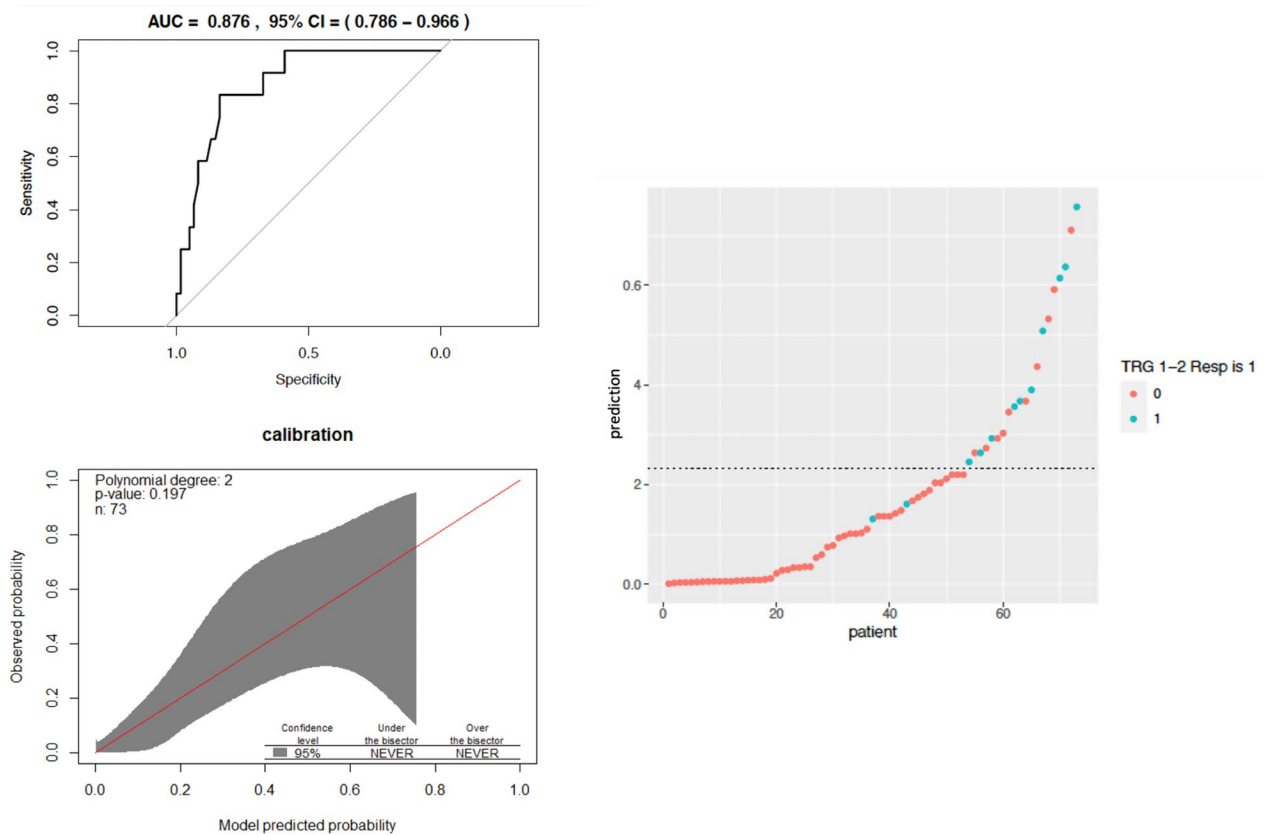


Fig. 2 Performance of the predictive model for major responders (TRG 1–2) to all types of chemotherapy. Panel A (top left): ROC curve; Panel B (right): the y-axis represents the probability of being major responders (TRG 1–2) predicted by the model for each patient – colors represent the true outcome, the dotted line represents the cut-off probability and classification threshold used to classify patients into major responders and non-major responders, patients with predicted probability above the cut-off are predicted as major responders (model-positives) and those with predicted probability below the cut-off are predicted as non-major responders (model-negative); panel C (bottom left): calibration belt

Table 3 Performance of the different models predicting the type of response to neoadjuvant chemotherapy

Model*	AUC (95% CI)	Accuracy (95% CI)	Se (95% CI)	Sp (95% CI)	PPV (95% CI)	NPV (95% CI)
MRs (TRG1-2 vs. 3–5)						
1. All types of chemotherapy (n=73) *radiomic/clinicopathologic	0.876 (0.786–0.966)	0.84 (0.73–0.91)	83 (56–96)	84 (73–91)	50 (29–71)	96 (88–99)
NRs (TRG1-3 vs. 4–5)						
1. All types of chemotherapy (n=77) *radiomic	0.725 (0.610–0.839)	0.70 (0.59–0.80)	72 (56–84)	68 (53–81)	70 (55–82)	70 (54–83)
2. ECF/EOX + FLOT (n=61) *radiomic	0.760 (0.639–0.882)	0.75 (0.63–0.86)	74 (57–87)	77 (60–89)	77 (60–89)	74 (57–87)
3. Oxaliplatin-based (n=53) *radiomic	0.810 (0.692–0.928)	0.77 (0.64–0.88)	96 (85–100)	56 (37–74)	71 (55–84)	93 (73–99)
4. FLOT (n=40) *radiomic	0.907 (0.818–0.995)	0.82 (0.67–0.93)	73 (52–88)	94 (77–99)	94 (76–99)	74 (54–88)

MRs: major responders; NRs: non-responders; TRG: tumor regression grade according to Mandard; AIUC: area under the curve; Se: sensitivity; Sp: specificity; PPV: positive predictive value, NPV: negative predictive value; ECF: epirubicin, cisplatin and fluorouracil; EOX: epirubicin, oxaliplatin and capecitabine; FLOT: fluorouracil, leucovorin, oxaliplatin and docetaxel; Oxaliplatin-based chemotherapy: FOLFOX (fluorouracil, leucovorin, oxaliplatin), EOX, FLOT

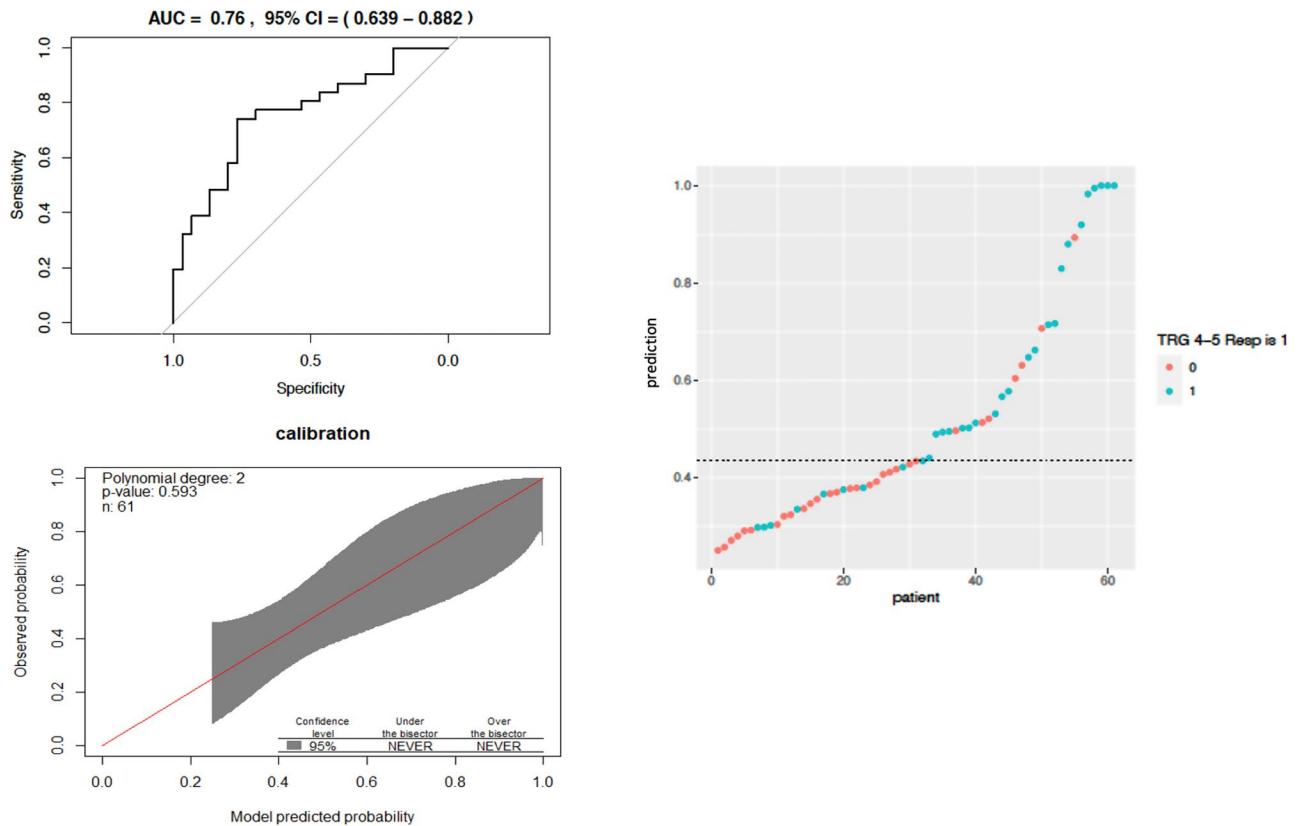


Fig. 3 Performance of the predictive model for non-responders (TRG 4–5) to ECF/EOX or FLOT chemotherapy. Panel A (top left): ROC curve; Panel B (right): the y-axis represents the probability of being non-responders (TRG 4–5) predicted by the model for each patient – colors represent the true outcome, the dotted line represents the cut-off probability and classification threshold used to classify patients into non-responders and not non-responders, patients with predicted probability above the cut-off are predicted as non-responders (model-positives) and those with predicted probability below the cut-off are predicted as not non-responders (model-negative); panel C (bottom left): calibration belt

[9–11]. Radiomics consists of the extraction of quantitative imaging features from imaging, to “decode” tissue characteristics and quantify other dimensional and morphological information. Radiomic features provide specific information about global gray-level histogram properties, local gray-scale patterns, inter-pixel relationships and shape within the regions of interest on radiological images and are successfully used to develop non-invasive prognostic and predictive models that may guide personalized diagnosis and treatment. For many tumor types, radiomic signatures have been related to specific tumor pathology aspects, and radiogenomic studies (those using radiomic models applied to genomics) have even reported a significant correlation of radiomic features with specific genes’ amplification status or mutations, improving treatment personalization performances [28, 29]. The role of the pathologic type and its microenvironment, as well as of its molecular/genomic signatures (i.e. HER2, MSI), have been regarded as possible determinants of prognosis and response to chemotherapy in GC and GEJC. Therefore, radiomics has a strong theoretical value, as an objective and low-cost method able to be integrated with other biomarkers for

better overall prediction or even to successfully integrate different types of information (i.e., imaging, pathologic, molecular, genomic) by itself.

In our study, features associated with response to chemotherapy all belonged to the statistical, textural, and morphological family. This means that relevant information was related to the variation and distribution of the gray levels within the tumor as well as its geometric properties. In particular, MR presented lower values for the 10th percentile of the intensity-histogram (“F_stat.10thpercentile”) compared to non-MR, as shown in Fig. 1. This feature represents a threshold that marks the point where the lowest 10% of the intensity values are located, identifying the relatively darker parts of the ROI and providing insights into tissue characteristics. On a similar note, NR presented higher values of the statistical feature “F_stat.energy” which is related to the magnitude of the gray-level values within the ROI. Higher values of this feature indicate that the pixel intensities within the tumor are more uniform and have more consistently high-intensity values, which could be associated with denser, more homogeneous tissue. This might be characteristic of highly cellular tumors, fibrotic regions, or solid

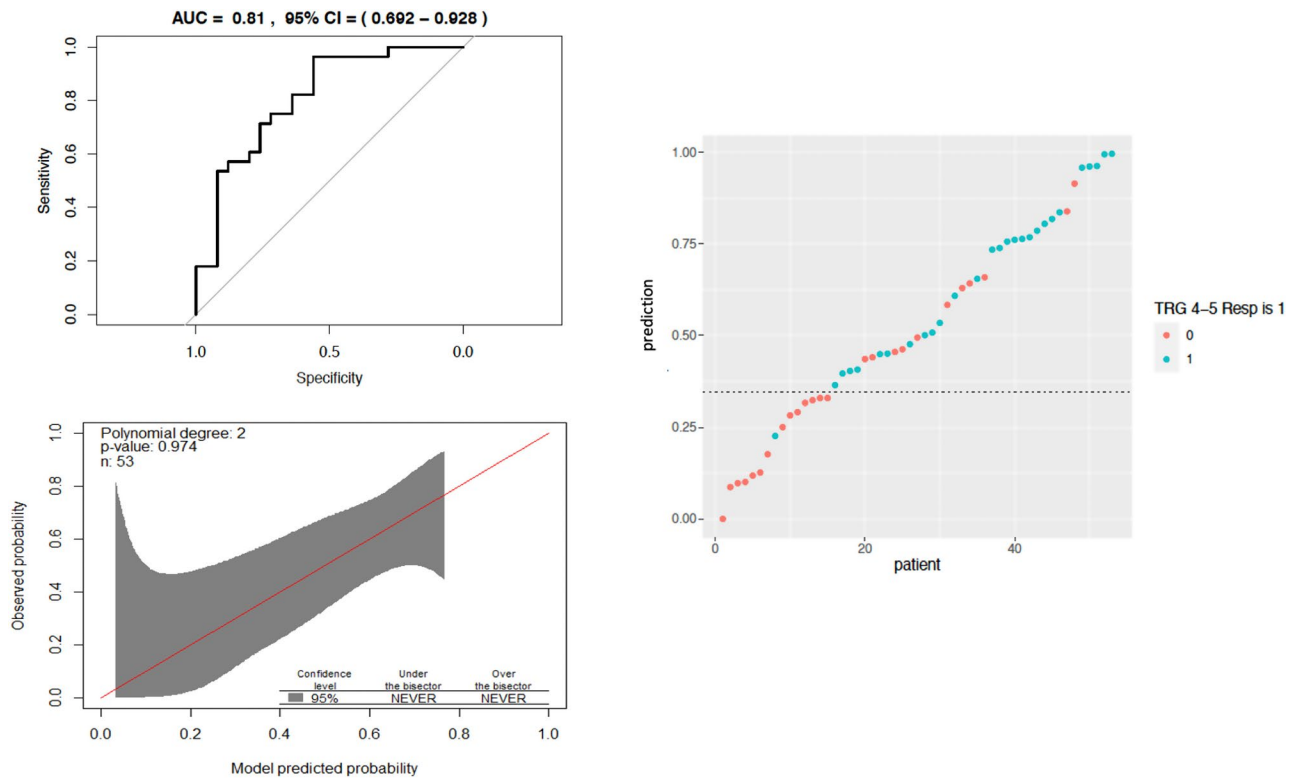


Fig. 4 Performance of the predictive model for non-responders (TRG 4–5) to oxaliplatin-based chemotherapy. Panel A (top left): ROC curve; Panel B (right): the y-axis represents the probability of being non-responders (TRG 4–5) predicted by the model for each patient – colors represent the true outcome, the dotted line represents the cut-off probability and classification threshold used to classify patients into non-responders and responders, patients with predicted probability above the dotted line are predicted as non-responders (model-positives) and those with predicted probability below the line are predicted as not non-responders (model-negative); panel C (bottom left): calibration belt

components of a lesion. NR also presented higher values of the morphological features “F_morph.volume” representing the tumor volume, lower values of the textural features “F_szm.hgze” and “F_szm_2.5D.szhge” emphasizing high gray levels and small zones sizes. Properties of the gray levels reflect the cellular and molecular characteristics of the tissues and could therefore be indicative of specific characteristics of the tumor microenvironment which are known prognostic and predictive factors for response to therapy in gastric cancer [30, 31], for example, the presence of immune infiltrates (typical of MSI and EBV-associated GC, with increased sensitivity to immunotherapy), or the tumor-stroma ratio (a lower tumor-stroma ratio has been detected in diffuse GC as well as in GC with epithelial-to-mesenchymal transition signatures, that are less susceptible to conventional chemotherapy) [32–36]. Morphology in terms of initial tumor volume has also been outlined as a predictor of response to chemotherapy in several tumor types [37, 38].

Only a few previous studies have to date investigated the role of radiomics in predicting the efficacy of neoadjuvant chemotherapy in gastric cancer. A large-scale Chinese study included 102 patients undergoing

neoadjuvant SOX regimen and investigated the correlation of a radiomic signature with pathologic MR, developing a model with good discrimination (AUC 0.82, CI 95% 0.67–0.98) and accuracy (Sp 88%, PPV 86%) and a significant correlation with survival [39]. Another recently published Chinese study, conducted on 292 patients who were administered the SEEOX and SOX regimens, developed a radiomic model for the prediction of downstaging that achieved promising outcomes in the external testing cohort of patients completing neoadjuvant therapy (AUC 0.750, CI 95% 0.579–0.921, accuracy 76.9%, Se 46.7% and Sp 95.8%) or undergoing early discontinuation of neoadjuvant chemotherapy (AUC 0.889, CI 95% 0.756–1, accuracy 83.7%, Se 57.1% and Sp 96.6%) [40].

In the Western setting, a first preliminary Italian study conducted on 34 patients detected a correlation between specific radiomic features and the status of NR to ECF neoadjuvant therapy [41]. Another recent Italian study from the GIRCG group conducted on 70 patients identified no correlation between pre-neoadjuvant therapy CT textural features and pathologic major response (TRG1 according to Becker) to different chemotherapy regimens [42]. Instead, promising results were obtained

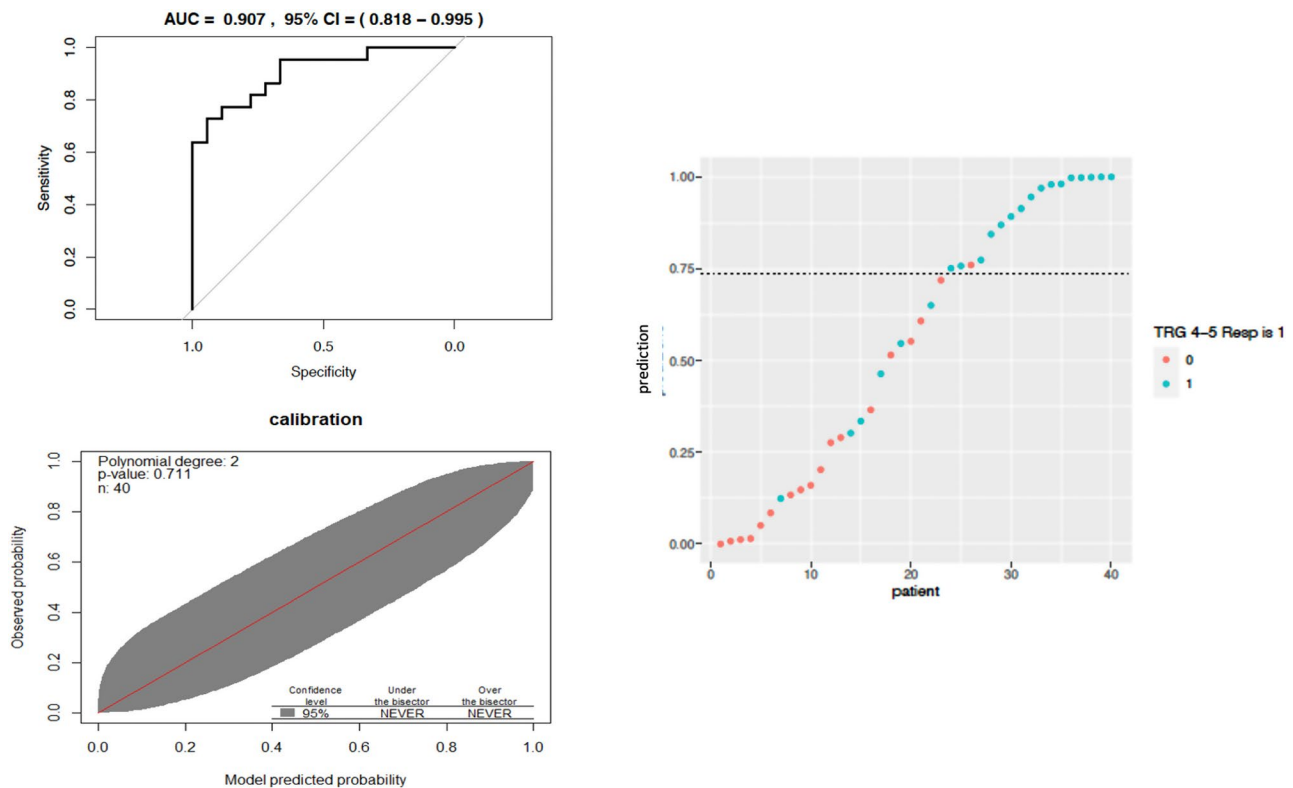


Fig. 5 Performance of the predictive model for non-responders (TRG 4–5) to FLOT chemotherapy. Panel A (top left): ROC curve; Panel B (right): the y-axis represents the probability of being non-responders (TRG 4–5) predicted by the model for each patient – colors represent the true outcome, the dotted line represents the cut-off probability and classification threshold used to classify patients into non-responders and not non-responders, patients with predicted probability above the dotted line are predicted as non-responders (model-positives) and those with predicted probability below the line are predicted as not non-responders (model-negative); panel C (bottom left): calibration belt

with delta radiomics, namely a type of radiomic analysis aimed to identify the change in radiomic features during or after treatment using images acquired at different time points. Our results are in line with the Eastern ones in identifying a correlation between pre-neoadjuvant therapy radiomic features and tumor pathologic response. In comparison with models derived from those studies, the ECF + FLOT, the oxaliplatin-based and the FLOT models in this study had an overall higher predictive performance. This may be due to the homogenous groups in terms of specific chemotherapy regimens, the choice of focusing on NR instead of MR, and/or the extraction of all the available radiomic feature families for the analysis, instead of just one family.

When comparing studies that used radiomics performed in the Eastern and Western settings, it should be considered that they are based on different approaches to the treatment of gastric cancer. In the Eastern setting, the use of neoadjuvant chemotherapy is indeed not the standard of care. Therefore, a model able to identify MR to chemotherapy would have the greatest clinical practice changing impact, allowing for the use of neoadjuvant chemotherapy instead of upfront surgery in a selected population. On the other hand, the use of neoadjuvant

chemotherapy currently represents the standard of care in the Western setting, where the greatest impact on clinical practice would be given by the possibility of identifying patients that have a high probability of not responding to chemotherapy, becoming able to address them to alternative medical treatments, or considering them for upfront surgery. These sectorial visions could be integrated into a global one, where an accurate predictive system may allow to screen MR, responders, and NR, allowing to plan different treatment plans for every category. Indeed, MR theoretically represent ideal candidates for a prolonged neoadjuvant regimen, aiming for a complete response, while responders could be better served by standard neoadjuvant chemotherapy followed by surgical resection. NR may instead be good candidates for alternative neoadjuvant chemotherapy regimens or upfront surgery with extended lymphadenectomy and/or implemented adjuvant support strategies (i.e., HIPEC, postoperative chemoradiotherapy, targeted treatments).

According to our results, given its high sensitivity (83%) and NPV (96%), the prediction model for MR appeared to be a valuable screening tool for “potential MR” that could be further tested (i.e., through more advanced delta radiomic models) and considered for

extended preoperative chemotherapy, although its immediate translational impact is still limited by heterogeneity of the chemotherapy regimens and relatively low positive predictive value (50%). Instead, the prediction models for NR for patients undergoing ECF + EOX, oxaliplatin-based, and FLOT chemotherapy had all good discrimination and accuracy. In particular, the FLOT model had a very high specificity and PPV (94% and 94%, respectively), representing a very low probability of incorrectly labeling patients as potential NR. These preliminary models, once further implemented and validated, could represent valuable decision support tools to identify candidates for different upfront approaches.

One limit of this study is its design (single-center, retrospective), which could have created potential biases due to the selection of patients and CT images based only on the available data in our institutional PACS, with a non-uniform interval between the diagnostic CT scan and the beginning of chemotherapy among the included patient, with some potential for variation in radiomic features across different imaging devices or protocols for image acquisition. This study was also limited by its small sample size and heterogeneity of the chemotherapeutic regimens. To reduce the impact of these issues, we applied a shrinkage approach for logistic regression and bootstrap resampling to control for overfitting providing a more realistic estimate of performance measures, according to recommendations specific for analyzing small sample sizes [16, 43, 44] and, when possible, we developed homogeneous models with regard of the administered chemotherapy. External validation of the models was not performed due to the exploratory, proof-of-concept aim of our study, therefore our results, although promising, cannot be deemed as generalizable. Lastly, the use of pathologic response as an outcome for the models could have led to an incorrect evaluation of the global clinical implications of the study. Indeed, the prognostic role of TRG is still not clearly established as, while most studies have found a significant correlation between the TRG and oncological outcomes [45–48], others have detected no association [49, 50] and suggested TRG to be a measure of locoregional response regardless of the presence of systemic micrometastatic disease [51].

Despite its limitations, this is one of the first studies applying radiomics for the prediction of response to the current standard-of-care regimen for perioperative chemotherapy, the FLOT, and other oxaliplatin-based regimens currently in use (i.e., the FOLFOX). Furthermore, the process of extracting radiomic features was realized by the IBSI initiative, in close cooperation with the radiologists attending the upper-GI multidisciplinary tumor board, representing a sound integration of the usual image analysis approach.

Within larger studies on the topic, it could be possible to yield a better understanding of the association of radiomic features with pathological features, and thoroughly investigate the role of specific features in determining the response to different chemotherapy regimens. In the future, we plan to implement and validate these models with multi-institutional recruitment of patients, correlation with long-term survival outcomes, and integration with clinicopathologic factors that were not available at the time of this study, as the molecular and genomic characterization of the tumor, or other laboratory-based biomarkers [52, 53], for boosting their translational impact and predictive accuracy, and implementing the early planning of a targeted multimodal treatment pathway for each GC and GEJC patient.

Conclusion

Overall, in this study, we developed a set of preliminary models, based on radiomic features extracted from the diagnostic CT scan of patients affected by GC and GEJC, to predict the response to different neoadjuvant chemotherapy strategies. The model for the prediction of MR had an overall good screening value for the identification of potential MR. The models predicting NR among patients undergoing ECF/EOX/FLOT, oxaliplatin-based chemotherapy, and FLOT had a satisfactory performance with good discrimination and accuracy. These radiomic models are promising and once further implemented on larger datasets, could be valuable instruments to target the multimodal treatment in patients with GC.

Supplementary Information

The online version contains supplementary material available at <https://doi.org/10.1186/s12957-025-03828-9>.

Supplementary Material 1

Acknowledgements

None.

Author contributions

A. A., L. B., F.P.: Conceptualization, Methodology, Data Analysis, Original draft preparation. H.E.T., M.G.B., R.R.: Data Analysis, Data curation, Writing-Original draft preparation. J.L., C.V., A.B.: Data interpretation, Literature review; Writing-Original draft preparation. R.M., V.V., D.D., R.P.: Data interpretation, Supervision, Writing-Reviewing and Editing. All authors read and approved the final manuscript.

Funding

None declared.

Data availability

No datasets were generated or analysed during the current study.

Declarations

Ethics approval and consent to participate

The study received approval from our Institutional Research Ethical Committee (Fondazione Policlinico Universitario A. Gemelli IRCCS ID 5297)

and was registered on clinicaltrials.gov (NCT06044961). All procedures were performed following the 1964 Helsinki Declaration and its later amendments.

Consent for publication

Informed consent for the treatment and data privacy and protection were obtained from all study participants.

Competing interests

The authors declare no competing interests.

Author details

¹Catholic University of the Sacred Heart, Largo F. Vito n.1, Rome 00168, Italy

²Department of Medical and Surgical Sciences, Fondazione Policlinico Universitario Agostino Gemelli IRCCS, Largo A. Gemelli n. 8, Rome 00168, Italy

³Department of Diagnostic Imaging, Oncological Radiotherapy and Hematology, Fondazione Policlinico Universitario "A. Gemelli" IRCCS, Largo A. Gemelli n. 8, Rome 00168, Italy

⁴Department of Women, Children and Public Health Sciences, Fondazione Policlinico Universitario Agostino Gemelli IRCCS, Largo A. Gemelli n. 8, Rome 00168, Italy

Received: 3 February 2025 / Accepted: 25 April 2025

Published online: 11 May 2025

References

1. Ychou M, Boige V, Pignon JP, Conroy T, Bouché O, Lebreton G, et al. Perioperative chemotherapy compared with surgery alone for resectable gastroesophageal adenocarcinoma: an FNCLCC and FFCD multicenter phase III trial. *J Clin Oncol*. 2011;29:1715–21. <https://doi.org/10.1200/JCO.2010.33.0597>.
2. Cunningham D, Allum WH, Stenning SP, Thompson JN, Van de Velde CJ, Nicolson M, et al. Perioperative chemotherapy versus surgery alone for resectable gastroesophageal cancer. *N Engl J Med*. 2006;355:11–20. <https://doi.org/10.1056/NEJMoa055531>.
3. Al-Batran SE, Homann N, Pauligk C, Goetze TO, Meiler J, Kasper S, et al. Perioperative chemotherapy with fluorouracil plus leucovorin, oxaliplatin, and docetaxel versus fluorouracil or capecitabine plus cisplatin and epirubicin for locally advanced, resectable gastric or gastro-oesophageal junction adenocarcinoma (FLOT4): a randomised, phase 2/3 trial. *Lancet*. 2019;393:1948–57. [https://doi.org/10.1016/S0140-6736\(18\)32557-1](https://doi.org/10.1016/S0140-6736(18)32557-1).
4. Li Z, Zhang D, Dai Y, Dong J, Wu L, Li Y, et al. Computed tomography-based radiomics for prediction of neoadjuvant chemotherapy outcomes in locally advanced gastric cancer: A pilot study. *Chin J Cancer Res*. 2018;30:406–14. <https://doi.org/10.21147/j.issn.1000-9604.2018.04.03.5>.
5. Al-Batran SE, Hofheinz RD, Pauligk C, Kopp HG, Haag GM, Luley KB, et al. Histopathological regression after neoadjuvant docetaxel, oxaliplatin, fluorouracil, and leucovorin versus epirubicin, cisplatin, and fluorouracil or capecitabine in patients with resectable gastric or gastro-oesophageal junction adenocarcinoma (FLOT4-AIO): results from the phase 2 part of a multicentre, open-label, randomised phase 2/3 trial. *Lancet Oncol*. 2016;17:1697–708. [https://doi.org/10.1016/S1470-2045\(16\)30531-9](https://doi.org/10.1016/S1470-2045(16)30531-9).
6. Cesario A, D'Oria M, Calvani R, Picca A, Pietragalla A, Lorusso D, et al. The role of artificial intelligence in managing Multimorbidity and Cancer. *J Pers Med*. 2021;11:314. <https://doi.org/10.3390/jpm11040314>.
7. Iwasaki Y, Terashima M, Mizusawa J, Katayama H, Nakamura K, Katai H, et al. Gastrectomy with or without neoadjuvant S-1 plus cisplatin for type 4 or large type 3 gastric cancer (JCOG0501): an open-label, phase 3, randomized controlled trial. *Gastric Cancer*. 2021;24:492–502. <https://doi.org/10.1007/s120-020-01136-7>.
8. Piessen G, Messager M, Le Malicot K, Robb WB, Di Fiore F, Guilbert M, et al. Phase II/III multicentre randomised controlled trial evaluating a strategy of primary surgery and adjuvant chemotherapy versus peri-operative chemotherapy for resectable gastric signet ring cell adenocarcinomas - PRODIGE 19 - FFCD1103 - ADICI002. *BMC Cancer*. 2013;13:281. <https://doi.org/10.1186/1471-2407-13-281>.
9. Cancer Genome Atlas Research Network. Comprehensive molecular characterization of gastric adenocarcinoma. *Nature*. 2014;513:202–9. <https://doi.org/10.1038/nature13480>.
10. Cristescu R, Lee J, Nebozhyn M, Kim KM, Ting JC, Wong SS, et al. Molecular analysis of gastric cancer identifies subtypes associated with distinct clinical outcomes. *Nat Med*. 2015;21:449–56. <https://doi.org/10.1038/nm.3850>.
11. Corso S, Giordano S. How can gastric cancer molecular profiling guide future therapies?? *Trends Mol Med*. 2016;22:534–44. <https://doi.org/10.1016/j.molmed.2016.05.004>.
12. Ko CC, Yeh LR, Kuo YT, Chen JH. Imaging biomarkers for evaluating tumor response: RECIST and beyond. *Biomark Res*. 2021;9:52. <https://doi.org/10.1186/s40364-021-00306-8>.
13. Lambin P, Leijenaar RTH, Deist TM, Peerlings J, de Jong EEC, van Timmeren J, et al. Radiomics: the Bridge between medical imaging and personalized medicine. *Nat Rev Clin Oncol*. 2017;14:749–62. <https://doi.org/10.1038/nrclinonc.2017.141>.
14. Li W, Zhang L, Tian C, Song H, Fang M, Hu C, et al. Prognostic value of computed tomography radiomics features in patients with gastric cancer following curative resection. *Eur Radiol*. 2019;29:3079–89. <https://doi.org/10.1007/s00330-018-5861-9>.
15. Li Q, Qi L, Feng QX, Liu C, Sun SW, Zhang J, et al. Machine Learning-Based computational models derived from Large-Scale Radiographic-Radiomic images can help predict adverse histopathological status of gastric cancer. *Clin Transl Gastroenterol*. 2019;10:e00079. <https://doi.org/10.14309/ctg.0000000000079>.
16. Moons KG, Altman DG, Reitsma JB, Ioannidis JP, Macaskill P, Steyerberg EW, et al. Transparent reporting of a multivariable prediction model for individual prognosis or diagnosis (TRIPOD): explanation and elaboration. *Ann Intern Med*. 2015;162:W1–73. <https://doi.org/10.7326/M14-0698>.
17. Biondi A, Agnes A, Del Coco F, Pozzo C, Strippoli A, D'Ugo D, et al. Preoperative therapy and long-term survival in gastric cancer: one size does not fit all. *Surg Oncol*. 2018;27:575–83. <https://doi.org/10.1016/j.suronc.2018.07.006>.
18. Carmona-Bayonas A, Jiménez-Fonseca P, Echavarría I, Sánchez Cánovas M, Aguado G, et al. Surgery for metastases for esophageal-gastric cancer in the real world: data from the AGAMENON National registry. *Eur J Surg Oncol*. 2018;44:1191–8. <https://doi.org/10.1016/j.ejso.2018.03.019>.
19. Zwanenburg A, Vallières M, Abdalah MA, Aerts HJWL, Andrearczyk V, Apte A, et al. The image biomarker standardization initiative: standardized quantitative radiomics for High-Throughput image-based phenotyping. *Radiology*. 2020;295:328–38. <https://doi.org/10.1148/radiol.2020191145>.
20. Dinapoli N, Alitto AR, Vallati M, Gatta R, Autorino R, Boldrini L, et al. Moddi-com: a complete and easily accessible library for prognostic evaluations relying on image features. *Annu Int Conf IEEE Eng Med Biol Soc*. 2015;2015:771–4. <https://doi.org/10.1109/EMBC.2015.7318476>.
21. Zhu Y, Sun Y, Hu S, Jiang Y, Yue J, Xue X, et al. Comparison of five tumor regression grading systems for gastric adenocarcinoma after neoadjuvant chemotherapy: a retrospective study of 192 cases from National Cancer center in China. *BMC Gastroenterol*. 2017;17:41. <https://doi.org/10.1186/s12876-017-0598-5>.
22. Kursu MB, Rudnicki WR. Feature Selection with the Boruta Package. *J. Stat. Soft.* [Internet]. 2010 [cited 2025 Mar. 31];36:1–13. Available from: <https://www.jstatsoft.org/index.php/jss/article/view/v036i11>
23. Firth D. Bias reduction of maximum likelihood estimates. *Biometrika*. 1993;80:27–38. <https://doi.org/10.1093/biomet/80.1.27>.
24. Brown LD, Cai TT, DasGupta A. Interval estimation for a binomial proportion. *Stat. Sci*. 2001;16: 101–117; <https://doi.org/10.1214/ss/1009213286>. Available from: <http://www.jstor.org/stable/267678423>
25. Nattino G, Lemeshow S, Phillips G, Finazzi S, Bertolini G. Assessing the calibration of dichotomous outcome models with the calibration belt. *Stata J*. 2018;17:1003–14. <https://doi.org/10.1177/1536867X1801700414>.
26. Matsuoka T, Yashiro M. Biomarkers of gastric cancer: current topics and future perspective. *World J Gastroenterol*. 2018;24:2818–32. <https://doi.org/10.3748/wjg.v24.i26.2818>.
27. Sato Y, Okamoto K, Kawaguchi T, Nakamura F, Miyamoto H, Takayama T. Treatment response predictors of neoadjuvant therapy for locally advanced gastric cancer: current status and future perspectives. *Biomedicines*. 2022;10:1614. <https://doi.org/10.3390/biomedicines10071614>.
28. Di Giannatale A, Di Paolo PL, Curione D, Lenkiewicz J, Napolitano A, Secinaro A, et al. Radiogenomics prediction for MYCN amplification in neuroblastoma: A hypothesis generating study. *Pediatr Blood Cancer*. 2021;68:e29110. <https://doi.org/10.1002/pbc.29110>.
29. Nero C, Ciccarone F, Boldrini L, Lenkiewicz J, Paris I, Capoluongo ED, et al. Germline BRCA 1–2 status prediction through ovarian ultrasound images radiogenomics: a hypothesis generating study (PROBE study). *Sci Rep*. 2020;10:16511. <https://doi.org/10.1038/s41598-020-73505-2>.

30. Jiang Y, Zhang Q, Hu Y, Li T, Yu J, Zhao L, et al. ImmunoScore signature: A prognostic and predictive tool in gastric Cancer. *Ann Surg.* 2018;267:504–13. <https://doi.org/10.1097/SLA.0000000000002116>.
31. Zhai J, Shen J, Xie G, Wu J, He M, Gao L, et al. Cancer-associated fibroblasts-derived IL-8 mediates resistance to cisplatin in human gastric cancer. *Cancer Lett.* 2019;454:37–43. <https://doi.org/10.1016/j.canlet.2019.04.002>.
32. Chen T, Li X, Mao Q, Wang Y, Li H, Wang C, et al. An artificial intelligence method to assess the tumor microenvironment with treatment outcomes for gastric cancer patients after gastrectomy. *J Transl Med.* 2022;20(1):100. <https://doi.org/10.1186/s12967-022-03298-7>.
33. Cai C, Hu T, Gong J, Huang D, Liu F, Fu C, et al. Multiparametric MRI-based radiomics signature for preoperative Estimation of tumor-stroma ratio in rectal cancer. *Eur Radiol.* 2021;31:3326–35. <https://doi.org/10.1007/s00330-020-07403-6>.
34. Meng Y, Zhang H, Li Q, Liu F, Fang X, Li J, et al. CT radiomics and Machine-Learning models for predicting Tumor-Stroma ratio in patients with pancreatic ductal adenocarcinoma. *Front Oncol.* 2021;11:707288. <https://doi.org/10.3389/fonc.2021.707288>.
35. Bos J, Groen-van Schooten TS, Brugman CP, Jamaludin FS, van Laarhoven HWM, Derks S. The tumor immune composition of mismatch repair deficient and Epstein-Barr virus-positive gastric cancer: A systematic review. *Cancer Treat Rev.* 2024;127:102737. <https://doi.org/10.1016/j.ctrv.2024.102737>.
36. Landeros N, Santoro PM, Carrasco-Avino G, Corvalan AH. Competing endogenous RNA networks in the epithelial to mesenchymal transition in Diffuse-Type of gastric Cancer. *Cancers (Basel).* 2020;12:2741. <https://doi.org/10.3390/cancers12102741>.
37. Partridge SC, Gibbs JE, Lu Y, Esserman LJ, Tripathy D, Wolverson DS, et al. MRI measurements of breast tumor volume predict response to neoadjuvant chemotherapy and recurrence-free survival. *AJR Am J Roentgenol.* 2005;184:1774–81. <https://doi.org/10.2214/ajr.184.6.01841774>.
38. Hill J, Yang F, Abraham A, Ghosh S, Steed TM, Kurtz C. Tumor volume predicts for pathological complete response in rectal cancer patients treated with neoadjuvant chemoradiation. *Int J Radiat Oncol Biol Phys.* 2021;111:e44. <https://doi.org/10.1016/j.ijrobp.2021.07.370>.
39. Sun KY, Hu HT, Chen SL, Ye JN, Li GH, Chen LD, et al. CT-based radiomics scores predict response to neoadjuvant chemotherapy and survival in patients with gastric cancer. *BMC Cancer.* 2020;20:468. <https://doi.org/10.1186/s12885-020-06970-7>.
40. Xu Q, Sun Z, Li X, Ye C, Zhou C, Zhang L, et al. Advanced gastric cancer: CT radiomics prediction and early detection of downstaging with neoadjuvant chemotherapy. *Eur Radiol.* 2021;31:8765–74. <https://doi.org/10.1007/s00330-021-07962-2>.
41. Giganti F, Marra P, Ambrosi A, Salerno A, Antunes S, Chiari D, et al. Pre-treatment MDCT-based texture analysis for therapy response prediction in gastric cancer: comparison with tumour regression grade at final histology. *Eur J Radiol.* 2017;90:129–37. <https://doi.org/10.1016/j.ejrad.2017.02.043>.
42. Mazzei MA, Di Giacomo L, Bagnacci G, Nardone V, Gentili F, Lucii G, et al. Delta-radiomics and response to neoadjuvant treatment in locally advanced gastric cancer—a multicenter study of GIRCG (Italian research group for gastric Cancer). *Quant Imaging Med Surg.* 2021;11:2376–87. <https://doi.org/10.21037/qims-20-683>.
43. Steyerberg EW, Eijkemans MJ, Habbema JD. Application of shrinkage techniques in logistic regression analysis: a case study. *Stat Neerl.* 2001;55:76–88.
44. Steyerberg EW, Harrell FE Jr, Borsboom GJ, Eijkemans MJ, Vergouwe Y, Habbema JD. Internal validation of predictive models: efficiency of some procedures for logistic regression analysis. *J Clin Epidemiol.* 2001;54:774–81. [https://doi.org/10.1016/s0895-4356\(01\)00341-9](https://doi.org/10.1016/s0895-4356(01)00341-9).
45. Tong Y, Zhu Y, Zhao Y, Shan Z, Liu D, Zhang J. Evaluation and comparison of predictive value of tumor regression grades according to Mandard and Becker in locally advanced gastric adenocarcinoma. *Cancer Res Treat.* 2021;53:112–22. <https://doi.org/10.4143/crt.2020.516>.
46. Lombardi PM, Mazzola M, Achilli P, Aquilano MC, De Martini P, Curaba A, et al. Prognostic value of pathological tumor regression grade in locally advanced gastric cancer: new perspectives from a single-center experience. *J Surg Oncol.* 2021;123:923–31.
47. Hayashi M, Fujita T, Matsushita H. Prognostic value of tumor regression grade following the administration of neoadjuvant chemotherapy as treatment for gastric/gastroesophageal adenocarcinoma: A meta-analysis of 14 published studies. *Eur J Surg Oncol.* 2021;47:1996–2003. <https://doi.org/10.1016/j.ejso.2020.12.010>.
48. Ikoma N, Estrella JS, Blum Murphy M, Das P, Minsky BD, Mansfield P, et al. Tumor regression grade in gastric Cancer after preoperative therapy. *J Gastrointest Surg.* 2021;25:1380–7. <https://doi.org/10.1007/s11605-020-04688-2>.
49. Bringeland EA, Wasmuth HH, Fougner R, Mjones P, Grønbech JE. Impact of perioperative chemotherapy on oncological outcomes after gastric cancer surgery. *Br J Surg.* 2014;101:1712–20. <https://doi.org/10.1002/bjs.9650>.
50. Blackham AU, Greenleaf E, Yamamoto M, Hollenbeak C, Gusani N, Coppola D, Pimiento JM, Wong J. Tumor regression grade in gastric cancer: predictors and impact on outcome. *J Surg Oncol.* 2016;114:434–9. <https://doi.org/10.1002/jso.24307>.
51. Mansour JC, Schwarz RE. Pathologic response to preoperative therapy: does it mean what we think it means? *Ann Surg Oncol.* 2009;16:1465–79. <https://doi.org/10.1245/s10434-009-0374-z>.
52. Chen YH, Xiao J, Chen XJ, Wang HS, Liu D, Xiang J, et al. Nomogram for predicting pathological complete response to neoadjuvant chemotherapy in patients with advanced gastric cancer. *World J Gastroenterol.* 2020;26:2427–39. <https://doi.org/10.3748/wjg.v26.i19.2427>.
53. Xu W, Ma Q, Wang L, He C, Lu S, Ni Z, et al. Prediction model of tumor regression grade for advanced gastric Cancer after preoperative chemotherapy. *Front Oncol.* 2021;11:607640. <https://doi.org/10.3389/fonc.2021.607640>.

Publisher's note

Springer Nature remains neutral with regard to jurisdictional claims in published maps and institutional affiliations.